Curvature and torsion feature extraction from free-form 3-D meshes at multiple scales

P.Yuen, F.Mokhtarian, N.Khalili and J.Illingworth

Abstract: A novel technique is presented for multi-scale curvature computation on a smoothed 3-D surface. This is achieved by convolving local parameterisations of the surface iteratively with 2-D Gaussian filters. In the technique, each vertex of the mesh becomes a local origin around which semi-geodesic co-ordinates are constructed. A geodesic from the origin is first constructed in an arbitrary direction, typically the direction of one of the incident edges. The smoothing eliminates surface noise and slowly erodes small surface detail, resulting in gradual simplification of the object shape. The surface Gaussian and mean curvature values are estimated accurately at multiple scales, together with curvature zero-crossing contours. For better visualisation, the curvature values are then mapped to colours and displayed directly on the surface. Furthermore local maxima of Gaussian and mean curvatures, as well as the torsion maxima of the zero-crossing contours of Gaussian and mean curvatures are also located and displayed on the surface. These features can be utilised by later processes for robust surface matching and object recognition. The technique is independent of the underlying triangulation and is more efficient than volumetric diffusion techniques since 2-D rather than 3-D convolutions are employed. Another advantage is that it is applicable to incomplete surfaces which arise during occlusion or to surfaces with holes.

1 Introduction

Curvature estimation is an important task in 3-D object description and recognition. Surface curvature provides a unique viewpoint invariant description of local surface shape. Differential geometry [1] provides several measures of curvature, which include Gaussian and mean curvatures. Combination of these curvature values enables the local surface type to be categorised.

In this paper, we introduce a new technique for multi-scale curvature computation on a smoothed 3-D surface. Complete triangulated models of 3-D objects are constructed and, using a local parameterisation technique, they are then smoothed using a 2-D Gaussian filter. The technique considered here is a generalisation of earlier multi-scale representation theories proposed for 2-D contours [2] and space curves [3]. However, note that the differential geometry of 3-D surfaces is significantly more complex than that of contours, and therefore this generalisation involves many non-trivial issues that do not arise in the earlier techniques. More details of the diffusion technique as well as a literature survey appear in [4].

In our approach, diffusion of the surface is achieved through convolutions of local parameterisations of the surface with a 2-D Gaussian filter [4, 5]. Semi-geodesic co-ordinates [1] are utilised as a natural and efficient way of locally parametrising surface shape. The most important advantage of our method is that, unlike other diffusion techniques such as volumetric diffusion [6, 7] or level set methods [8], it has local support and is therefore applicable to partial data corresponding to surface segments. This property makes it suitable for object recognition applications in the presence of occlusions. It is also more efficient than those techniques since 2-D rather than 3-D convolutions are employed.

Using this approach, we show examples of 3-D objects with their estimated Gaussian and mean curvature values [1]. For visualisation, the curvature values on the surface can be mapped to colours [9]. Once surface curvatures are estimated, curvature zero-crossing contours are recovered and displayed on the surface. Local maxima of Gaussian and mean curvatures, as well as the maxima of torsion of zero-crossing contours of Gaussian and mean curvatures, are also located and displayed on the surface.

2 Literature survey

Many object recognition systems rely on restrictions imposed on the geometry of the object. However, complex free-form surfaces may not be modelled easily using volumetric primitives. A free-form surface is a surface such that the surface normal is defined and continuous everywhere, except at sharp corners and edges [10]. Discontinuities in the surface normal or curvature may be present anywhere on a free-form object. The curves that connect these points of discontinuity may meet or diverge smoothly. Recognition of free-form objects is essential in inspection of arbitrary curved surfaces and in path planning for robot navigation.

In this Section, we present a survey of previous work on representation of 3-D surfaces. Sinha and Jain [11] provide an overview of geometry-based representations derived

IEE Proceedings online no. 20000487

DOI: 10.1049/ip-vis:20000487

Paper first received 5th July 1999 and in revised form 24th March 2000

The authors are with the Centre for Vision, Speech, and Signal Processing, School of Electronic Engineering, Information Technology and Mathematics, University of Surrey, Guildford GU2 5XH, UK

from range data of objects. Comprehensive surveys of 3-D object recognition systems are presented by Besl and Jain [12], Chin and Dyer [13] and Suetens *et al.* [14]. Several representation schemes for 3-D objects have adopted some form of surface or volumetric parametric models to characterise the shape of the objects. Current volumetric representations rely on representing objects in terms of generalised cylinders, superquadrics, set-theoric combinations of volume primitives as in constructive solid geometry (CSG) or spatial occupancy [15–19]. However, it may not be possible to express all objects with free-form surfaces using a single scheme such as superquadric primitives. Although there are several methods available to model a surface, triangular meshes are the simplest and most used form of polygon to cover a free-form surface. Common types of polygonal mesh include the triangular mesh [20–22] and the four-sided spline patches. Triangular meshes have been utilised in our work.

Polyhedral approximations [23] model an object using vertices and flat faces. Their disadvantage is that the process which determines the vertices is not robust to noise and local deformations of shape. Smooth 3-D splines [24] can also be fitted to 3-D objects. Their shortcomings are that the process of knot point selection is again not robust and that the spline parameters are not invariant. Generalised cones or cylinders [25] and geons [26] approximate a 3-D object using globally parametrised mathematical models, but they are not applicable to detailed free-form objects. Multi-view representations [27] are based on a large number of views of a 3-D object obtained from different viewpoints, but difficulties can arise when a new view is encountered. In volumetric diffusion [7] or level set methods [8], an object is treated as a filled area or volume. The object is then blurred by processes described by the classic diffusion equation. The boundary of each blurred object can then be defined by applying the Laplacian operator to the smoothed area or volume. The major shortcoming of these approaches is lack of local support. In other words, the entire object must be available. This problem makes them unsuitable for object recognition in the presence of occlusion. A form of 3-D surface smoothing has been suggested previously [28, 29], but this method has drawbacks since it is based on weighted averaging using neighbouring vertices and is therefore dependent on the underlying triangulation. The smoothing of 3-D surfaces is a result of the diffusion process [30]. For parameterisation of a 3-D surface, other methods have been studied, such as the use of asymptotic co-ordinates [31], isothermic co-ordinates [1, 32] and global co-ordinates [33], as used for closed simply connected objects.

Another approach for specifying a 3-D object is a view-centred representation. The aspect graph approach [34] attempts to take the infinite set of 2-D views of a 3-D object and partition it into a small set of representative or typical views. Murase and Nayar [35] use this approach, together with photometric information, to describe and recognise objects. A major drawback of view-centred representations is the lack of complete information.

Recent approaches using point set based registration [36], splash and super polygonal segments [37] and algebraic polynomials [38, 39] have addressed the issue of representing complex curved free-form surfaces. However, there are limitations relating to object segmentation issues, surface fitting convergence, restricting objects to be topologically equivalent to a sphere, and sensitivity to noise when low-level surface features are used.

3 Semi-geodesic parametrisation

Free-form 3-D surfaces are complex; hence no global co-ordinate system exists on these surfaces which could yield a natural parametrisation of the surface. Studies of local properties of 3-D surfaces are carried out in differential geometry using local co-ordinate systems called curvilinear co-ordinates or Gaussian co-ordinates [1]. Each system of curvilinear co-ordinates is introduced on a patch of a regular surface referred to as a simple sheet. A simple sheet of a surface is obtained from a rectangle by stretching, squeezing, and bending, but without tearing or gluing together. Given a parametric representation $\boldsymbol{r} = \boldsymbol{r}(u, v)$ on a local patch, the values of the parameters u and v determine the position of each point on that patch. Construction and implementation of semi-geodesic co-ordinates in our technique is described in [4].

3.1 Geodesic lines and semi-geodesic co-ordinates

A geodesic line is defined as a contour which locally represents the shortest distance on a 3-D surface between any two points on that contour. A semi-geodesic co-ordinate system consists of two families of co-ordinate lines which are mutually perpendicular. In our method, an initial geodesic line is drawn arbitrarily through the origin of the local area. This geodesic line is sampled at equal-sized intervals, based on the average length of triangle edges. The second family of lines are also geodesic lines and normals to the first line at the sampled points. All the lines together form semigeodesic co-ordinates.

3.2 Geodesic line construction

Before semigeodesic co-ordinates can be defined on a local patch at a chosen vertex V, an arbitrary geodesic line must be constructed. The edge connecting V and one of its neighbouring vertices is selected as an arbitrary direction. Since the surface is locally represented as a flat polyhedral facet, a straight line is a geodesic, and this can be followed until an edge or vertex is reached. This new edge point or vertex becomes a starting point for the next extension. To continue a geodesic line into the next triangle, we first measure the angle between the line and the edge common to both triangles which is intersected by the geodesic line. We then extend the line into the next triangle at the same angle. The construction of this geodesic line continues until the last edge or vertex of the local area is reached. The same process is used to construct the negative portion of the geodesic line.

3.3 Perpendicular geodesic line construction

The second family of lines are constructed perpendicularly to the above geodesic line. At each sampled point of the geodesic line, a perpendicular geodesic line is constructed. Using a similar technique to that described in Section 3.2. the perpendicular lines are constructed in the forward direction, as well as the backward direction, with respect to the geodesic line. This completes the construction of a local semigeodesic parametrisation.

Semigeodesic co-ordinates can also be constructed at or near a boundary in the case of an incomplete surface or a surface with holes. In such cases, geodesic lines are constructed as before, but they are terminated as soon as they intersect the surface boundary. Fig. 1 shows the complete semigeodesic co-ordinates on a triangular mesh.

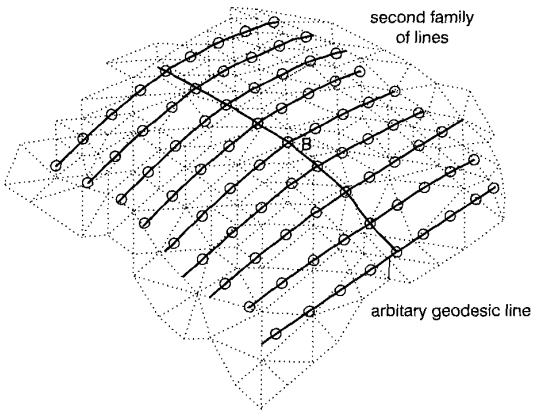

Fig. 1 *Semi-geodesic co-ordinates on triangular mesh*

3.4 2-D Gaussian convolution

Gaussian filtering is a weighted average smoothing carried out at a vertex and its neighbourhood. A 2-D Gaussian filter is generated according to the formula below [40]:

$$G(u, v, \sigma) = \frac{1}{2\pi\sigma^2} e^{-\frac{(u^2+v^2)}{2\sigma^2}} \quad (1)$$

The spatial extent of the Gaussian filter is determined by the variance σ, and this can be set to include only vertices in a small area local to the vertex. For a large 3-D surface, smoothing is achieved by using many fixed size local filters. To avoid over- or under-sampling, the size of the area must be carefully chosen. In other words, a local area must be a reasonably large size to provide accurate results but cannot be too large: otherwise it yields invalid results, as semigeodesic co-ordinates are only defined locally. Experiments conducted with a filter size of 9 with $\sigma = 1.0$ yielded the most reasonable results.

To smooth a 3-D surface, a fixed size 2-D Gaussian filter with $\sigma = 1.0$ is convolved with the local area. Local parametrisation of the surface yields

$$r(u, v) = (x(u, v), y(u, v), z(u, v)) \quad (2)$$

The smooth surface is defined by

$$R(u, v, \sigma) = (\mathcal{X}(u, v, \sigma), \mathcal{Y}(u, v, \sigma), \mathcal{Z}(u, v, \sigma)) \quad (3)$$

where

$$\mathcal{X}(u, v, \sigma) = x(u, v) * G(u, v, \sigma)$$
$$\mathcal{Y}(u, v, \sigma) = y(u, v) * G(u, v, \sigma)$$
$$\mathcal{Z}(u, v, \sigma) = z(u, v) * G(u, v, \sigma)$$

and * denotes convolution. This process is repeated at each vertex, and the new vertex positions after filtering define the smoothed surface. This procedure is iterated several times to achieve multi-scale smoothing of the surface.

4 Curvature estimation

In this Section, we present techniques for accurate estimation of Gaussian and mean curvatures at multiple scales on smoothed free-form 3-D surfaces. Differential geometry provides several measures of curvature, which include Gaussian and mean curvatures [1]. Consider a local parametric representation of a 3-D surface

$$\boldsymbol{r} = \boldsymbol{r}(u, v)$$

with co-ordinates u and v, where

$$\boldsymbol{r}(u, v) = (x(u, v), y(u, v), z(u, v))$$

Gaussian curvature K exists at regular points of a surface of class C_2. To define Gaussian curvature, we first consider the concept of the spherical image. The spherical image of a point P on a surface is a point on the unit sphere with the same normal vector. Now consider a domain Ω on the surface, which contains the point P. Let Ω^* be the spherical image of Ω. Take the ratio of the area of Ω^* to the area of Ω. The limit as the domain Ω contracts to P of this ratio is called the Gaussian curvature of the surface at P. When $\boldsymbol{r}(u, v)$ corresponds to semigeodesic co-ordinates, K is given by

$$K = \frac{b_{uu}b_{vv} - b_{uv}^2}{x_v^2 + y_v^2 + z_v^2} \quad (4)$$

where subscripts denote partial derivatives, and

$$b_{uu} = \frac{Ax_{uu} + By_{uu} + Cz_{uu}}{\sqrt{A^2 + B^2 + C^2}}$$
$$b_{vv} = \frac{Ax_{vv} + By_{vv} + Cz_{vv}}{\sqrt{A^2 + B^2 + C^2}}$$
$$b_{uv} = \frac{Ax_{uv} + By_{uv} + Cz_{uv}}{\sqrt{A^2 + B^2 + C^2}}$$

where

$$A = y_u z_v - z_u y_v \quad B = x_v z_u - z_v x_u \quad C = x_u y_v - y_u x_v$$

Mean curvature H also exists at regular points of a surface of class C_2. Mean curvature at a point P of a surface is defined as the arithmetic mean of the principal curvatures at point P. The principal curvatures at a point P of a surface are the largest and smallest values of normal curvatures for all directions at point P. Finally, the normal curvature at P of a curve on a surface is the projection of the curvature vector of the curve at P on the normal vector of the surface at P. When $\boldsymbol{r}(u, v)$ corresponds to semi-geodesic co-ordinates, H is given by

$$H = \frac{b_{vv} + (x_v^2 + y_v^2 + z_v^2)b_{uu}}{2(x_v^2 + y_v^2 + z_v^2)} \quad (5)$$

The mathematical properties of the two surface curvature functions are now discussed in more detail. Both Gaussian and mean curvature values are direction-free quantities. Gaussian and mean curvatures are invariant to arbitrary transformation of the (u, v) parameters, as well as rotations and translations of a surface. Combination of these curvature measures enables the local surface type to be categorised. On smoothed surfaces of 3-D objects, the procedure for estimating the Gaussian and mean curvatures is as follows. For each point of the surface,

$$p(x(u, v), y(u, v), z(u, v))$$

the corresponding local neighbourhood data are convolved with the partial derivatives of the Gaussian function $G(u, v, \sigma)$, i.e.

$$x_u = x * \frac{\partial G}{\partial u}, \quad y_u = y * \frac{\partial G}{\partial u}, \quad z_u = z * \frac{\partial G}{\partial u}$$
$$x_v = x * \frac{\partial G}{\partial v}, \quad y_v = y * \frac{\partial G}{\partial v}, \quad z_v = z * \frac{\partial G}{\partial v}$$
$$x_{uu} = x * \frac{\partial^2 G}{\partial u^2}, \quad y_{uu} = y * \frac{\partial^2 G}{\partial u^2}, \quad z_{uu} = z * \frac{\partial^2 G}{\partial u^2}$$
$$x_{vv} = x * \frac{\partial^2 G}{\partial v^2}, \quad y_{vv} = y * \frac{\partial^2 G}{\partial v^2}, \quad z_{vv} = z * \frac{\partial^2 G}{\partial v^2}$$
$$x_{uv} = x * \frac{\partial^2 G}{\partial u \partial v}, \quad y_{uv} = y * \frac{\partial^2 G}{\partial u \partial v}, \quad z_{uv} = z * \frac{\partial^2 G}{\partial u \partial v}$$

where * denotes convolution. Finally, curvature values on a 3-D surface are estimated by substituting these values into equations 4 and 5, respectively.

4.1 Curvature zero-crossing contours

After computing curvature values at each vertex of a smoothed 3-D surface, we can locate curvature zero-crossing contours, where curvature functions K or H (defined by eqns. 4 and 5) are equal to zero. Curvature zero-crossing contours can be useful for segmenting a smoothed 3-D surface into regions. The process of recovery of the curvature zero-crossing contours is identical for Gaussian and mean curvatures. Every edge e of the smoothed surface is examined in turn. If the vertices at each end of e have the same signs of curvature, then there is no curvature zero-crossing point on e. However, if the vertices of e have different signs of curvature, then there exists a point on e at which curvature goes to zero. The zero-crossing point is assumed to be at the midpoint of e. The other two edges of the triangle to which e belongs are then checked, since there must be another zero-crossing point on one of those edges. When that zero-crossing is found, it is connected to the previously found zero-crossing. The curvature zero-crossing contour is tracked in this fashion until we return to the starting point.

4.2 Local curvature maxima

Local maxima of Gaussian and mean curvatures are significant and robust feature points on smoothed surfaces, since noise has been eliminated from those surfaces. The process of recovery of the local maxima is identical for Gaussian and mean curvatures. Every vertex V of the smoothed surface is examined in turn. The neighbours of V are defined as vertices that are connected to V by an edge. If the curvature value of V is greater than the curvature values of all its neighbours, V is marked as a local maximum of curvature. Curvature maxima can be utilised by later processes for robust surface matching and object recognition with occlusion.

4.3 Maxima of torsion of curvature zero-crossing contours

In this Section, we review the computation of torsion. Torsion is the instantaneous rate of change of the osculating plane with respect to the arc length parameter. The osculating plane at a point P is defined to be the plane with the highest order of contact with the curve at P. Formally, let P be a regular point of a curve of class C_3, and let Q be a variable point on the curve in a small neighbourhood of P. Let P correspond to the value s of the arc length parameter and Q to the value $s+h$. Denote by ψ the angle from the osculating plane at P to the osculating plane at Q. The limit of the ratio ψ/h as $h \rightarrow 0$ is called the torsion of the curve at P. Intuitively, torsion is a local measure of the nonplanarity of a space curve [1]. The set of points of a space curve are the values of a continuous, vector-valued, locally one-to-one function

$$r(u) = (x(u), y(u), z(u))$$

where $x(u)$, $y(u)$ and $z(u)$ are the components of $r(u)$, and u is a function of arc length of the curve. To compute torsion τ at each point of the curve, it is expressed in terms of the derivatives of $x(u)$, $y(u)$ and $z(u)$. In case of an arbitrary parametrisation, torsion is given by

$$\tau = \frac{\dot{x}(\dot{y}\ddot{z} - \ddot{z}\ddot{y}) - \dot{y}(\dot{x}\ddot{z} - \ddot{z}\dot{x}) + \dot{z}(\dot{x}\ddot{y} - \ddot{y}\dot{x})}{(\dot{y}\ddot{z} - \dot{z}\ddot{y})^2 + (\dot{z}\ddot{x} - \dot{x}\ddot{z})^2 + (\dot{x}\ddot{y} - \dot{y}\ddot{x})^2} \quad (6)$$

where $\dot{x}(u)$, $\dot{y}(u)$ and $\dot{z}(u)$ are the convolutions of $x(u)$, $y(u)$ and $z(u)$ with the first derivative of a 1-D Gaussian function $G_1(u, \sigma)$

$$\dot{x} = x * \frac{\partial G_1}{\partial u}, \quad \dot{y} = y * \frac{\partial G_1}{\partial u}, \quad \dot{z} = z * \frac{\partial G_1}{\partial u}$$

where * denotes convolution. Note that $\ddot{x}$ and $\dddot{x}$ represent convolutions with the second and third derivatives of G_1.

5 Results and discussion

In this Section, we present results on free-form surface smoothing, as well as curvature estimation.

5.1 Diffusion

The smoothing routines were implemented entirely in C++. Complete triangulated models of 3-D objects used in our experiments were constructed through fusion of multiple range images [21, 22]. To experiment with our techniques, both simple and complex 3-D objects with different numbers of triangles were used. Each iteration of smoothing of a surface with 1000 vertices took about 0.5 second of CPU time on an UltraSparc 170E.

The first test object was a toy dinosaur model, with 2996 triangles and 1500 vertices, as shown in Fig. 2. Note that the surface noise was eliminated iteratively, with the object becoming smoother gradually. The legs, tail and ears were removed after 10 iterations. The next test object was a cow, with 3348 triangles and 1676 vertices, as shown in Fig. 3. The surface noise was eliminated iteratively, with the object becoming smoother gradually. After 12 iterations the legs, ears and tail were removed (as was seen for the dinosaur).

These examples show that our technique is effective in eliminating surface noise as well as removing surface detail. The result is gradual simplification of object shape. Note that our technique is robust to mesh geometry and structure. This is achieved by uniform sampling of the mesh surface when semi-geodesic co-ordinates are constructed. In fact, we applied decimation to the mesh after each iteration of smoothing to remove odd-shaped triangles. However, this procedure did not have any adverse effects on the results.

Owing to the local nature of semi-geodesic co-ordinates, our technique is also applicable to incomplete surfaces which arise during occlusion or surfaces with holes. Because of space constraints the corresponding results could not be included here. The interested reader is referred to [5].

Our technique has been tested on several datasets representing complex shapes, and the results indicate the robustness of the technique under various conditions of noise and shape deformations. For further examples of smoothing, see [4, 41].

5.2 Curvature estimation

In this Section, we present the results of application of our curvature estimation techniques to 3-D objects using methods described in Section 4. The first example is the dinosaur. After smoothing the object, the Gaussian curvatures of all vertices were estimated. To visualise these curvature values on the surface, they were mapped to

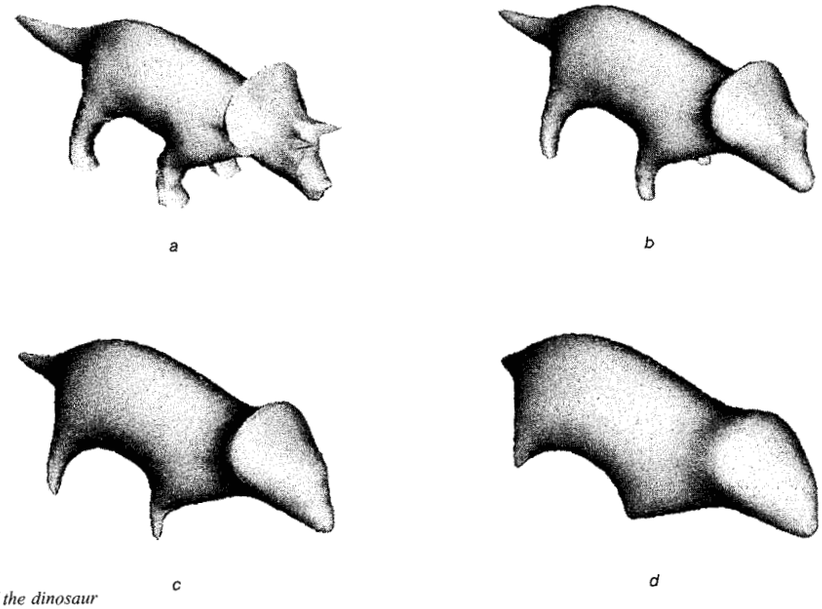

Fig. 2 *Smoothing of the dinosaur*
a Original
b 3 iterations
c 5 iterations
d 10 iterations

colours using the Visualisation Toolkit (VTK) [9]. The results are shown in Figs. 4*a* and *b*. Surface curvature colours are coded as follows: red = high, blue = low, and green = non-extreme values. All convex corners of the dinosaur are red, indicating high curvature values; the concave corners are blue, indicating low curvature values; and other areas are green, since their curvature values are close to zero. The same experiment was repeated to estimate the mean curvatures of the dinosaur, and the results are shown in Figs. 4*c* and *d*. The next object was a cow, and the Gaussian and mean curvatures were also estimated, and Fig. 5 shows the results.

The curvature zero-crossing contours of these surfaces were found and displayed on the surface. Curvature zero-crossing contours can be used for segmenting surfaces into regions. Figs. 6*a* and *b* show Gaussian curvature zero-crossing contours for the smoothed dinosaur. Figs. 6*c* and *d* show mean curvature zero-crossing contours for the same object. The same experiments were repeated for the cow, and these results are shown in Fig. 7. Note that the number

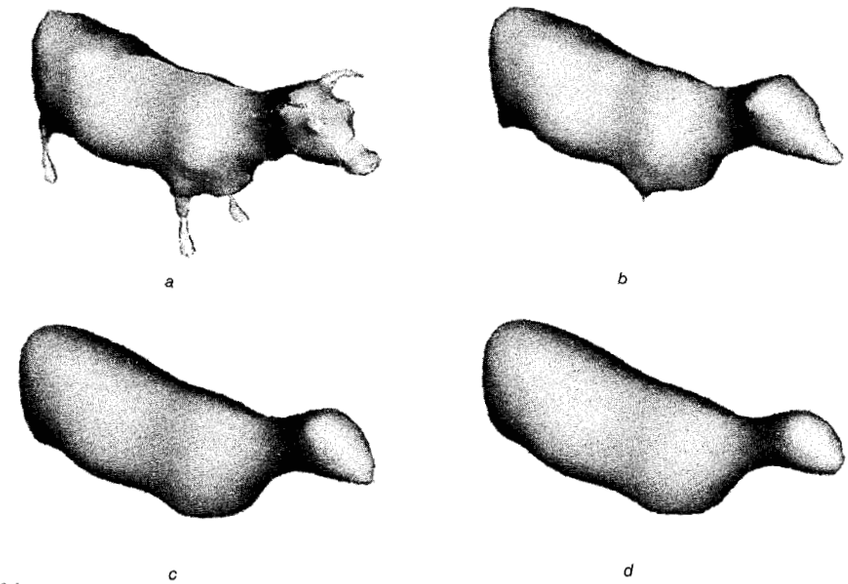

Fig. 3 *Smoothing of the cow*
a Original
b 3 iterations
c 8 iterations
d 12 iterations

Fig. 4 *Gaussian (top row) and mean (bottom row) curvatures on the dinosaur*
a One iteration
b 6 iterations
c One iteration
d 6 iterations

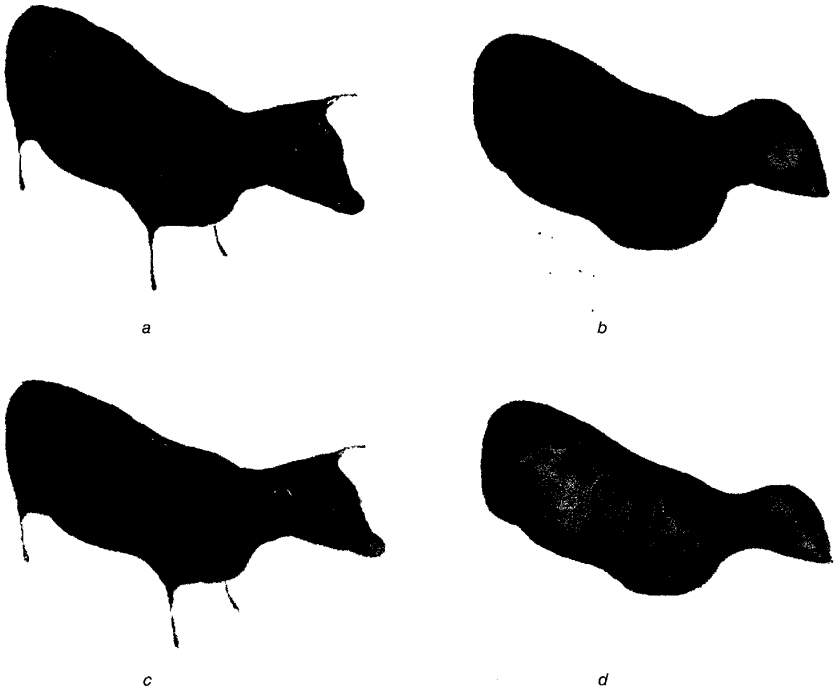

Fig. 5 *Gaussian (top row) and mean (bottom row) curvatures on the cow*
a One iteration
b 6 iterations
c One iteration
d 6 iterations

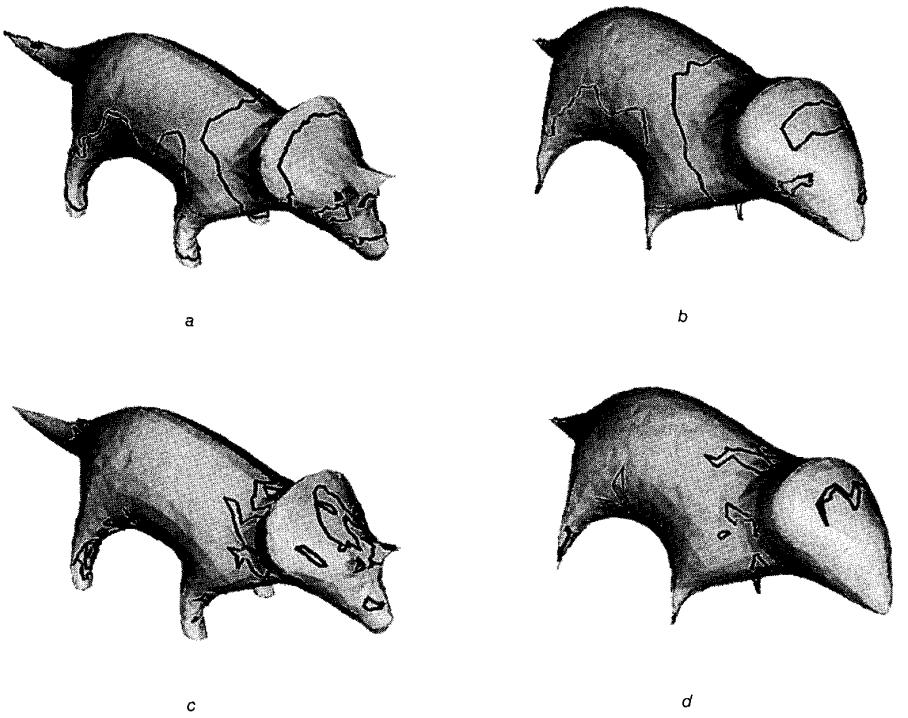

Fig. 6 *Gaussian (top row) and mean (bottom row) curvature zero-crossing contours on the dinosaur*
a One iteration
b 6 iterations
c One iteration
d 6 iterations

of curvature zero-crossing contours is reduced as the object is smoothed iteratively.

From the curvature values, the local curvature maxima for the smoothed objects can be computed. The local maxima of Gaussian curvature on the dinosaur are shown in Fig. 8*a*. Fig. 8*b* shows the local maxima of mean curvature. The local maxima of Gaussian and mean curvatures for the cow are shown in Fig. 9. All curvature maxima are shown after one iteration.

Finally, the torsion maxima of curvature zero-crossing contours, which are alternative features used for matching, were determined and displayed on the object. Figs. 10*a* and *b* show the torsion maxima of curvature zero-crossing contours of the dinosaur for Gaussian and mean curvatures,

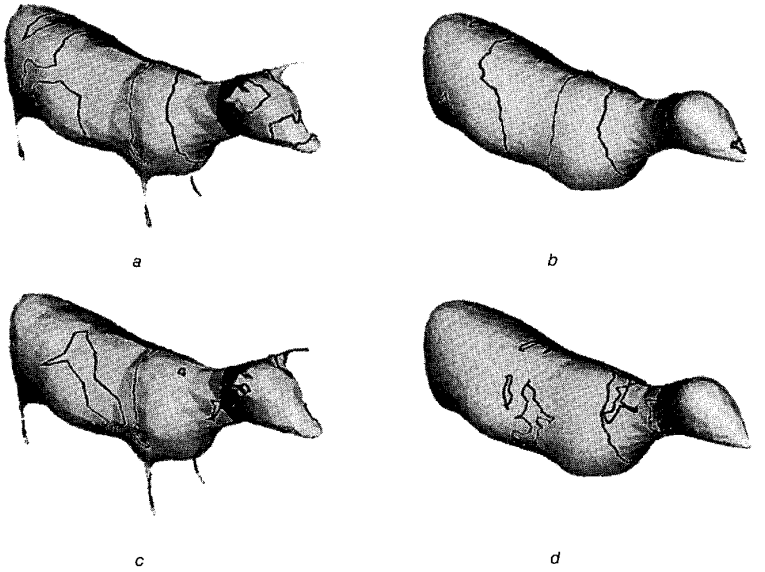

Fig. 7 *Gaussian (top row) and mean (bottom row) curvature zero-crossing contours on the cow*
a One iteration
b 6 iterations
c One iteration
d 6 iterations

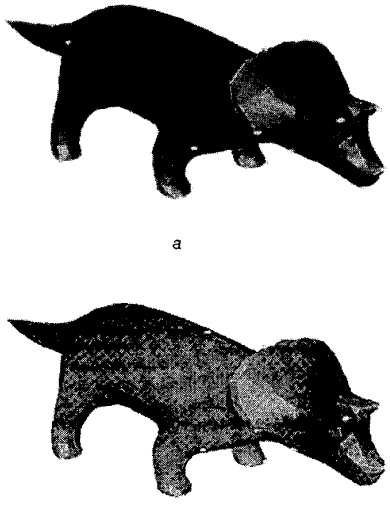

Fig. 8 *Curvature maxima of the dinosaur*
a Gaussian
b Mean

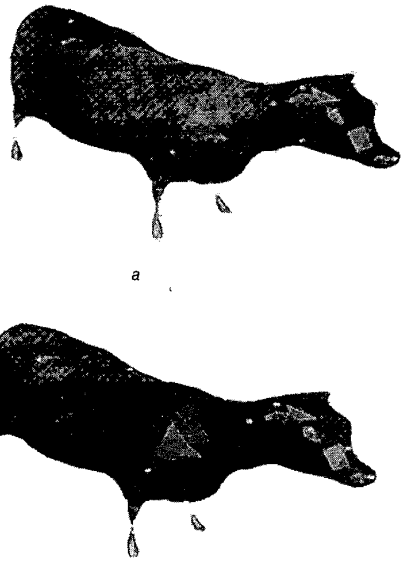

Fig. 9 *Curvature maxima of the cow*
a Gaussian
b Mean

respectively. Fig. 11 shows the results for the cow. The torsion maxima are also shown after one iteration.

These features can be utilised by later processes for robust surface matching and object recognition with occlusion. Animation of surface diffusion can be observed at our web site: *http://www.ee.surrey.ac.uk/Research/VSSP/demos/css3d/index.html*

6 Conclusions

A novel technique for multi-scale curvature computation on a smoothed 3-D surface has been presented. In our technique, each vertex of the mesh becomes the local

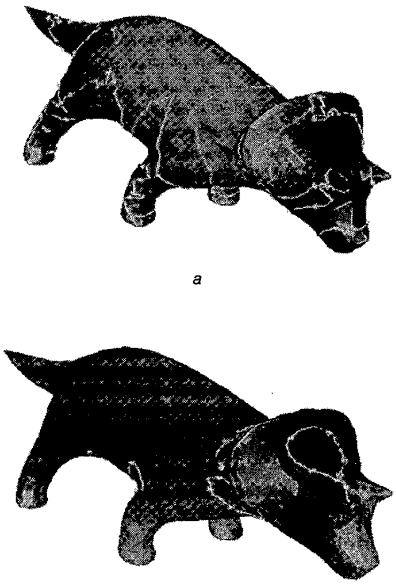

Fig. 10 *Torsion maxima of curvature zero-crossing contours of the dinosaur*
a Gaussian
b Mean

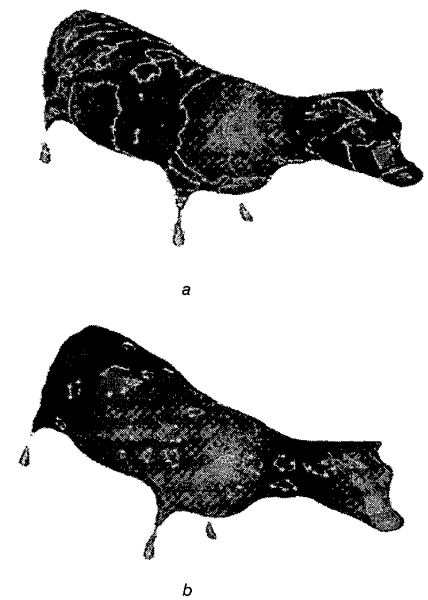

Fig. 11 *Torsion maxima of curvature zero-crossing contours of the cow*
a Gaussian
b Mean

origin around which semi-geodesic co-ordinates are constructed. A geodesic from the origin is constructed in an arbitrary direction, such as the direction of one of the incident edges. During the smoothing process, 3-D surfaces are sampled locally using different step sizes. Complete triangulated models of 3-D objects are constructed and, using a local parametrisation technique, are then smoothed using a 2-D Gaussian filter. The smoothing eliminated the surface noise and small surface detail gradually, and resulted in gradual simplification of object shape. The surface Gaussian and mean curvatures

were also estimated. To visualise these curvature values on the surface, they are then mapped to colours and shown directly on the surface. All convex corners of the surface indicated high Gaussian curvature values, whereas the concave corners indicated low Gaussian curvature values and the curvature values of flat areas are close to zero.

Gaussian and mean curvature zero-crossing contours were also recovered and displayed on the surface. Results indicated that as the surface is smoothed iteratively, the number of curvature zero-crossing contours is reduced. Curvature zero-crossing contours can be used for segmenting surfaces into regions. Furthermore, the local maxima of Gaussian and mean curvatures, as well as the torsion maxima of zero-crossing contours of Gaussian and mean curvatures, were located and displayed on the surface. These features can be used by later processes for robust surface matching and object recognition with occlusion.

7 References

1 GOETZ, A.: 'Introduction to differential geometry' (Addison-Wesley, Reading, Massachussetts, 1970)

2 MOKHTARIAN, F., and MACKWORTH, A.K.: 'A theory of multi-scale, curvature-based shape representation for planar curves', *IEEE Trans. Patt. Anal. Mach. Intell.*, 1992, **14**, (8), pp. 789–805

3 MOKHTARIAN, F.: 'A theory of multi-scale, torsion-based shape representation for space curves', *Computer Vis. Image Underst.*, 1997, **68**, (1), pp. 1–17

4 MOKHTARIAN, F., KHALILI, N., and YUEN, P.: 'Multi-scale 3-D free-form surface smoothing'. Proceedings of British Machine Vision Conf., 1998, pp. 730–739

5 YUEN, P., MOKHTARIAN, F., and KHALILI, N.: 'Multi-scale 3-D surface description: open and closed surfaces'. Proceedings of Scandinavian Conf. on *Image Analysis*, 1999, Greenland, pp. 303–310

6 KOENDERINK, J.J., and VANDOORN, A.J.: 'Dynamic shape', *Biol. Cybernet.*, 1986, **53**, pp. 383–396

7 KOENDERINK, J.J.: 'Solid shape' (MIT Press, Cambridge, Massachussetts, 1990)

8 SETHIAN, J.A.: 'Level set methods' (Cambridge University Press, 1996)

9 SCHROEDER, W., MARTIN, K., and LORENSEN, B.: 'The visualization toolkit: an object oriented approach to 3-D graphics' (Prentice Hall, 1996)

10 BESL, P.J.: 'The free-form surface matching problem', *in* FREEMAN, H. (Ed.): 'Machine vision for three-dimensional scenes' (1990), pp. 25–71

11 SINHA, S.S., and JAIN, R.: 'Range image analysis', *in* YOUNG, T.Y. (Ed.): 'Handbook of pattern recognition and image processing: computer vision', **2**, 1994, pp. 185–237

12 BESL, P.J., and JAIN, R.C.: 'Three dimentional object recognition', *ACM Comput. Surv.*, 1985, **17**, pp. 75–145

13 CHIN, R.T., and DYER, C.R.: 'Model-based recognition in robot vision', *ACM Comput. Surv.*, 1986, **18**, (1), pp. 67–108

14 SUETENS, P., FUA, P., and HANSON, A.J.: 'Computational strategies for object recognition', *ACM Comput. Surv.*, 1992, **24**, (2), pp. 45–61

15 BROOKS, R.A.: 'Model-based three-dimensional interpretations of two-dimensional images', *IEEE Trans. Patt. Anal. Mach. Intell.*, 1983, **5**, pp. 140–150

16 CHEN, T.W., and LIN, W.C.: 'A neural network approach to CSG-based 3-D object recognition', *IEEE Trans. Patt. Anal. Mach. Intell.*, 1994, **16**, (7), pp. 719–726

17 PENTLAND, A.P.: 'Perceptual organisation and the representation of natural form', *Artif. Intell.*, 1986, **28**, pp. 293–331

18 SOLINA, F., and BAJCSY, R.: 'Recovery of parametric models from range images: The case for superquadrics with global deformations', *IEEE Trans. Patt. Anal. Mach. Intell.*, 1990, **12**, pp. 131–147

19 SAMET, H.: 'The design and analysis of spatial data structures' (Addison-Wesley, 1990)

20 HILTON, A., STODDART, A.J., ILLINGWORTH, J., and WINDEATT, T.: 'Marching triangles: range image fusion for complex object modelling'. Proceedings of IEEE Int. Conf. on *Image Processing*, 1996, Lausanne, Switzerland, pp. 381–384

21 HILTON, A., STODDART, A.J., ILLINGWORTH, J., and WINDEATT, T.: 'Reliable surface reconstruction from multiple range images'. Proceedings of European Conf. on *Computer Vision*, 1996, Cambridge, UK, pp. 117–126

22 HILTON, A., STODDART, A.I., ILLINGWORTH, J., and WINDEATT, T.: 'Implicit surface based geometric fusion', *Comput. Vis. Image Underst. (Special Issue on CAD based vision)*, 1998, **69**, (3), pp. 273–291

23 FAUGERAS, O.D., and HEBERT, M.: 'The representation, recognition, and locating of 3-D object', *Int. J. Robotics Res.*, 1986, **5**, (3), pp. 27–52

24 STODDART, A.J., and BAKER, M.: 'Reconstruction of smooth surfaces with arbitrary topology adaptive splines'. Proceedings of European Conf. on *Computer Vision*, 1998, **II**, pp. 241–254

25 SOROKA, B.I., and BAJCSY, R.K.: 'Generalized cylinders from serial sections'. Proceedings of Int. Joint Conf. on *Pattern Recognition*, 1976, pp. 734–735

26 PILU, M., and FISHER, R.: 'Recognition of geons by parametric deformable contour models'. Proceedings of European Conf. on *Computer Vision*, 1996, Cambridge, UK, pp. 71–82

27 SEIBERT, M., and WAXMAN, A.M.: 'Adaptive 3-D object recognition from multiple views', *IEEE Trans. Patt. Anal. Mach. Intell.*, 1992, **14**, pp. 107–124

28 TAUBIN, G.: 'Curve and surface smoothing without shrinkage'. Proceedings of Int. Conf. on *Computer Vision*, 1995, pp. 852–857

29 TAUBIN, G., ZHANG, T., and GOLUB, G.: 'Optimal surface smoothing as filter design'. Proceedings of European Conf. on *Computer Vision*, 1996, pp. 283–292

30 TER HAAR ROMENY, B.M.: 'Geometry driven diffusion in computer vision' (Kluwer Academic, 1994)

31 KREYSZIG, E.: 'Differential geometry' (Oxford University Press, 1959)

32 CHERN, S.S., HARTMAN, P., and WINTNER, A.: 'On isometric coordinates, *in* 'Commentaries mathematical Helvetici' **28**, (1954)

33 BRECHBUHLER, C., GERIG, G., and KUBLER, O.: 'Parametrization of closed surfaces for 3-D shape description', *Computer Vis. Image Underst.*, 1995, **61**, (2), pp. 154–170

34 KOENDERINK, J.J., and VANDOORN, A.J.: 'Internal representation of solid shape with respect to vision', *Biol. Cybernet.*, 1979, **32**, (4), pp. 211–216

35 MURASE, H., and NAYAR, S.K.: 'Visual learning and recognition of 3-D objects from appearance', *Int. J. Computer Vis.*, 1995, **14**, (1), pp. 5–24

36 BESL, P.J., and MCKAY, N.D.: 'A method for registration of 3-D shapes', *IEEE Trans. Patt. Anal. Mach. Intell.*, 1992, **14**, (2), pp. 239–256

37 STEIN, F., and MEDIONI, G.: 'Structural indexing: efficient 3-D object recognition', *IEEE Trans. Patt. Anal. Mach. Intell.*, 1992, **14**, pp. 125–145

38 KEREN, D., COPPER, D., and SUBRAHMONIA, J.: 'Describing complicated objects by implicit polynomials', *IEEE Trans. Patt. Anal. Mach. Intell.*, 1994, **16**, pp. 38–53

39 PONCE, J., KRIEGMAN, D.J., PETITJAAN, S., SULLIVAN, S., TAUBIN, G., and VIJAYAKUMAR, B.: 'Representations and algorithms for 3-D curved object recognition', *in* 'Three-dimensional object recognition systems' (Amsterdam, Netherlands, 1993), pp. 17–56

40 BANKS, S.P.: 'Signal Processing, Image Processing and Pattern Recognition' (Prentice-Hall, 1990)

41 KHALILI, N., MOKHTARIAN, F., and YUEN, P.: 'Free-form surface description in multiple scales: Extension to incomplete surfaces'. Proceedings of Int. Conf. on *Computer Analysis of Images and Patterns*, 1999, Slovenia, Ljubljana, pp. 293–300